



EurJIC

European Journal of Inorganic Chemistry

 **Chemistry
Europe**

European Chemical
Societies Publishing

Accepted Article

Title: Catalytic Disproportionation of Hydrazine Promoted by Biomimetic Diiron Complexes with Benzene-1,2-Dithiolate Bridge Modified by Different Substituents

Authors: Tie Sun, Sunlin Xu, Dawei Yang, Linan Su, Baomin Wang, and Jingping Qu

This manuscript has been accepted after peer review and appears as an Accepted Article online prior to editing, proofing, and formal publication of the final Version of Record (VoR). This work is currently citable by using the Digital Object Identifier (DOI) given below. The VoR will be published online in Early View as soon as possible and may be different to this Accepted Article as a result of editing. Readers should obtain the VoR from the journal website shown below when it is published to ensure accuracy of information. The authors are responsible for the content of this Accepted Article.

To be cited as: *Eur. J. Inorg. Chem.* 10.1002/ejic.202000851

Link to VoR: <https://doi.org/10.1002/ejic.202000851>

WILEY-VCH

Catalytic Disproportionation of Hydrazine Promoted by Biomimetic Diiron Complexes with Benzene-1,2-Dithiolate Bridge Modified by Different Substituents

Tie Sun,^[a] Sunlin Xu,^[a] Dawei Yang,^{*[a]} Linan Su,^[a] Baomin Wang^[a] and Jingping Qu^{[a][b]}

A series of thiolate-bridged diiron nitrogenase mimics featuring benzene-1,2-dithiolate (bdt) ligand modified by different substituents were synthesized and characterized by X-ray crystallography. Electrochemical studies by cyclic voltammetry demonstrate the redox potentials of these complexes depend on the electron-withdrawing or electron-donating nature of different substituents. Importantly, all these complexes can serve as catalysts for disproportionation of hydrazine to ammonia and dinitrogen, wherein the complex with the most negative reduction potential induced by

strong electron-donating NMe₂ group exhibits the best catalytic activity. This result bodes well for efficient catalyst design for N–N bond cleavage of hydrazine. In addition, a well-defined diiron diazene complex can be independently synthesized and also catalyze the hydrazine disproportionation to ammonia. However, relatively low yield suggests this species may not be a key intermediate during the catalytic cycle unlike the other reported bimetallic systems.

Introduction

Elucidating the detailed mechanism of nitrogen reduction catalyzed by nitrogenases is a fascinating and challenging task for biologists and chemists for decades,^[1] which is essential to the development of mild catalysts for ammonia synthesis. To date, for the question that how many metals participate in nitrogen fixation, there are two assumptions: one involves N₂ binding to one Mo or Fe atom, whereas the other suggests two or more iron atoms located in the “belt” region of the FeMo-cofactor are responsible for the coordination and activation of nitrogen.^[2] Recently, biochemical studies in the spectroscopy and structure of the FeMo-cofactor under turnover state reveal that the “belt” diiron centers are likely to be the genuine active site.^[3] Therefore, it is of great importance to construct dinuclear iron-sulfur clusters as nitrogenase mimics and explore their reactivity toward dinitrogen and other nitrogenous substrates such as diazene (N₂H₂), hydrazine (N₂H₄), which provides some key information to understand the activation mode of substrates at a molecular level.

Hydrazine is not only regarded as a four-electron and proton reduced intermediate species during nitrogen reduction process,^[4] but also a potential substrate of nitrogenases.^[5] Nitrogenases catalyze the N–N bond cleavage of hydrazine at the late stage of nitrogen reduction process possibly through reduction or disproportionation pathways.^[6] So far, many transition metal complexes can realize the catalytic reduction

and disproportionation of hydrazine.^[7–13] However, most of them involve early transition metals including molybdenum,^[7] tungsten^[8] and vanadium^[9] or heteronuclear di- or multi-metallic centers^[12] and only a handful of biomimetic iron-sulfur complexes are reported.^[13] For instance, a thiolate-bridged diiron phenyl diazene complex reported by our group can accomplish the catalytic N–N bond cleavage of hydrazine and its derivatives in the presence of proton and reductant.^[13a] Besides, Peters and co-workers reported a mono-thiolate bridged diiron complex that can mediate catalytic disproportionation of hydrazine to ammonia and dinitrogen.^[13c]

Benzene-1,2-dithiolate (bdt) as a common redox non-innocent ligand has drawn considerable attention in the chemical community.^[14] Extensive research has shown that the modification of the substituent on the bdt ligand can affect catalytic activity by changing the redox potential of metallic complexes.^[15] In our previous work, we also adopted bdt as a bridging ligand to construct a novel diiron nitrogenase mimic [Cp*Fe(μ - η^2 : η^4 -bdt)FeCp*] (Cp* = η^5 -C₅Me₅) (**1a**), which can systematically simulate the biological nitrogen fixation process through the transformation of N₂H₂ → N₂H₃ → NH(+NH₃) → NH₂ → NH₃.^[16] In this biomimetic [Fe₂S₂] scaffold, the binding flexibility of the bdt ligand is crucial to the accommodation of a series of N_xH_y species. However, there is no report about the catalytic transformation of N₂ and other nitrogenous substrates such as N₂H₄ using this system.

To get a deep understanding of its electronic effect on the catalytic reactivity, herein we report the synthesis, characterization, and catalytic activity of a class of bdt-bridged diiron complexes by introducing different substituents into the phenyl of the bdt ligand. Of particular note, these complexes all can catalytically disproportionate hydrazine to ammonia and dinitrogen, which is significantly related to their distinct redox properties.

[a] T. Sun, S. Xu, Dr. D. Yang, Dr. L. Su, Prof. B. Wang, Prof. J. Qu
State Key Laboratory of Fine Chemicals
Dalian University of Technology
Dalian, 116024, P. R. China
E-mail: yangdw@dlut.edu.cn
URL: http://faculty.dlut.edu.cn/yangdawei/zh_CN/

[b] Prof. J. Qu
Key Laboratory for Advanced Materials
East China University of Science and Technology
Shanghai, 200237, P. R. China

Supporting information

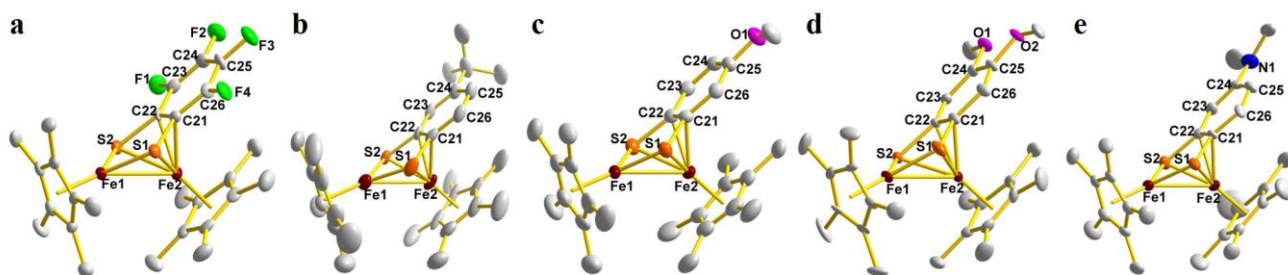


Figure 1. Oak ridge thermal ellipsoid plot (ORTEP) diagrams of complexes **1b** (a), **1c** (b), **1d** (c), **1e** (d) and **1f** (e) drawn by diamond software at 50% probability level. The hydrogen atoms on all carbon atoms are omitted for clarity.

Table 1. Main bond lengths (Å) and angles (deg) in complexes **1a-1f**.

Complex	1a ^[16]	1b	1c	1d	1e	1f
Fe1–Fe2	2.7635(4)	2.7589(10)	2.7778(12)	2.7750(9)	2.7780(4)	2.7649(8)
Fe1–S1	2.1447(6)	2.1372(15)	2.182(3)	2.1495(14)	2.1462(7)	2.212(2)
Fe1–S2	2.1466(6)	2.1379(15)	2.132(3)	2.1421(15)	2.1493(7)	2.1041(19)
Fe2–S1	2.2940(6)	2.2897(15)	2.296(2)	2.3005(14)	2.2931(6)	2.367(2)
Fe2–S2	2.2950(6)	2.2948(15)	2.265(3)	2.2896(14)	2.2952(6)	2.2157(19)
Fe2–C21	2.092(2)	2.068(5)	2.112(7)	2.117(5)	2.106(2)	2.174(6)
Fe2–C22	2.103(2)	2.076(5)	2.103(8)	2.084(5)	2.097(2)	2.12(2)
S1–C21	1.769(2)	1.771(5)	1.754(8)	1.768(5)	1.763(2)	1.762(7)
S2–C22	1.769(2)	1.762(5)	1.774(10)	1.758(5)	1.770(2)	1.77(2)
Fe1–Cp*1	1.6641(3)	1.6633(6)	1.654(1)	1.6622(8)	1.6791(4)	1.6587(6)
Fe2–Cp*2	1.6711(3)	1.6677(9)	1.6754(7)	1.6848(6)	1.6703(3)	1.6600(5)
Fe1–S1S2–Fe2	118.11(3)	119.10 (8)	119.05(13)	118.16 (6)	118.59(3)	116.5(1)
Cp*1–Cp*2	62.79(7)	61.75 (20)	61.9(2)	60.8(4)	61.2(3)	62.14(15)

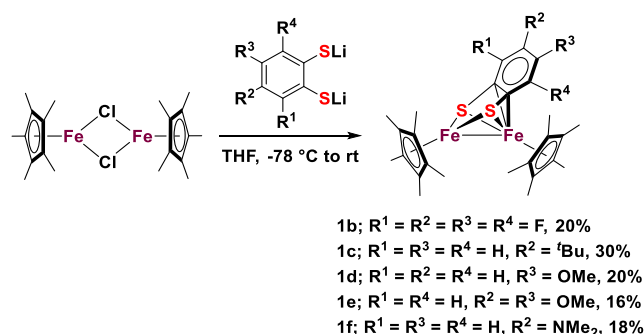
Results and Discussion

Synthesis, characterization and structure of thiolate-bridged diiron complexes [Cp*Fe(μ - η^2 : η^4 -bdt^R)FeCp*]

Initially, in order to examine the substituent effect on the biomimetic catalytic activity, electron-withdrawing or electron-donating groups were introduced into the redox non-innocent bdt ligand of the original thiolate-bridged diiron nitrogenase mimic **1a**.^[16] Using a general procedure as outlined in **Scheme 1**, treatment of precursor [Cp*FeCl]₂ with 1 equiv. of Li₂bdt^R (R = F, ^tBu, OMe, NMe₂) in THF from -78 °C to room temperature generated a series of thiolate-bridged diiron complexes [Cp*Fe(μ - η^2 : η^4 -bdt^R)FeCp*] (**1b**, R¹ = R² = R³ = R⁴ = F; **1c**, R¹ = R³ = R⁴ = H, R² = ^tBu; **1d**, R¹ = R² = R⁴ = H, R³ = OMe; **1e**, R¹ = R⁴ = H, R² = R³ = OMe; **1f**, R¹ = R³ = R⁴ = H, R² = NMe₂) as a microcrystalline powder. These complexes were all characterized by proton nuclear magnetic resonance (¹H NMR), infrared spectrum (IR), elemental analysis and X-ray diffraction crystallographic analysis.

The ¹H NMR spectroscopic results indicate all these complexes should be diamagnetic species. Notably, the resonances for the two Cp* ligands are broad, but there is no paramagnetic shift observed. This result may be attributed to the slight magnetic disturbance of the iron centers. When the substituent is electron-withdrawing, the signal for Cp* of **1b** appears at 1.67 ppm, which slightly shifts upfield compared with the unmodified complex **1a** (1.71 ppm). On the contrary, when

the substituent is electron-donating, the corresponding signals shift downfield as observed at 1.76, 1.76 and 1.81 ppm for complexes **1c**, **1d** and **1f**, respectively. Unexpectedly, there are two broad peaks for the two Cp* ligands in the ¹H NMR spectrum of complex **1e** in C₆D₆ at room temperature. However, if using THF-d₈ as deuterium solvent, there is only a very broad peak for the two Cp* ligands. When the temperature lowered, this broad resonance can gradually split into two sharp peaks (**Figure S13**), which suggests the shuttle of the phenyl group between the diiron centers in the solution state is thermally dependent.



Scheme 1. Synthesis of complexes **1b-1f**

Furthermore, the molecular structures of complexes **1b-1f** were unambiguously determined by X-ray single-crystal diffraction analysis as shown in **Figure 1**. The main bond lengths and angles are summarized in **Table 1**, which reveal that the $[\text{Fe}_2\text{S}_2]$ unit of diiron complexes are similar in metrical parameters. Similar to complex **1a**, the modified bdt ligands in complexes **1b-1f** also lean towards one iron center and bind to the two iron centers in a $\mu\text{-}\eta^2\text{:}\eta^4$ coordination fashion, which lead to an unsymmetrical geometric arrangement. The Fe1–Fe2 bond lengths of complexes **1b-1f** fall in a narrow range from 2.7589(10) to 2.7780(4) Å, which indicates the slight enhancement and weakening of the metal-metal bonding interaction due to the introduction of different types of substituents compared with **1a** (2.7635(4) Å). Because the two carbon atoms adjacent to sulfur atoms are π -bonded to the electron-deficient iron center in **1b-1f**, the Fe2–S1 and Fe2–S2 bonds are obviously weakened and longer than the Fe1–S1 and Fe1–S2 bonds. Notably, when the phenyl ring of the bdt ligand was mono-substituted as observed in **1c**, **1d** and **1f**, the Fe1–S1, Fe1–S2 and Fe2–S1, Fe2–S2 bond lengths are remarkably distinct. These changes of Fe–S bond length caused by substituents have also been found in other reported metal thiolate complexes.^[14] The C23–C24 and C25–C26 bond distances are shorter than others in the phenyl ring, which suggests the modified bdt ligands are still π -radical mono-anionic as in complex **1a**.^[16,17] In addition, electron-donating substituents also lead to the elongation of Fe2–C21 bond, revealing the weaker π coordination interaction between iron and bdt^R ligand. These structural differences among these complexes may have an impact on their catalytic properties.

Electrochemical studies of complexes **1b-1f**

Next, we investigated the redox behaviors of complexes **1b-1f** by cyclic voltammetry (CV) to get deep insight into the potential influence of substituents of the modified bdt ligand. As shown in **Figure 2**, the CV curves of complexes **1b-1f** all display a reversible one-electron reduction event, which is assigned to the $\text{Fe}^{\text{II}}\text{Fe}^{\text{II}}/\text{Fe}^{\text{II}}\text{Fe}^{\text{I}}$ redox couple.^[18] When all hydrogen atoms in the bdt ligand were substituted by electron-withdrawing fluoride, the reductive half-wave potential ($E_{1/2}^{\text{red}}$) for $\text{Fe}^{\text{II}}\text{Fe}^{\text{II}}/\text{Fe}^{\text{II}}\text{Fe}^{\text{I}}$ couple of **1b** is -0.402 V versus ferrocene ($\text{Fc}^{+/0}$), which is 92 mV more positive than that of **1a**. The electron-donating inductive effect of the *tert*-butyl group in complex **1c** is responsible for a significant shift of $E_{1/2}^{\text{red}}$ toward negative potential ($E_{1/2}^{\text{red}} = -0.848$ V, 354 mV more negative than **1a**). Unexpectedly, the negative shift of redox couple caused by the $-\text{NMe}_2$ group in complex **1f** ($E_{1/2}^{\text{red}} = -0.920$ V) is even more visible than that of **1e** with two methoxy groups ($E_{1/2}^{\text{red}} = -0.883$ V). It can be speculated that increasing the electron-donating ability of the bdt ligand would enrich the electron density in the diiron centers and lower the reduction potential of these complexes.

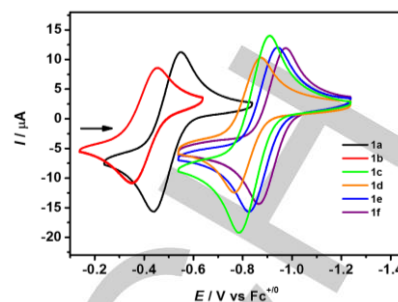
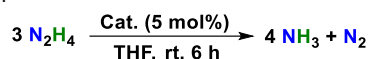


Figure 2. Cyclic voltammograms of complexes **1a-1f**, measured in 0.1 M $^t\text{Bu}_4\text{NPF}_6$ in CH_2Cl_2 at 100 mV/s and internally referenced to Fc^+/Fc .

Catalytic hydrazine disproportionation

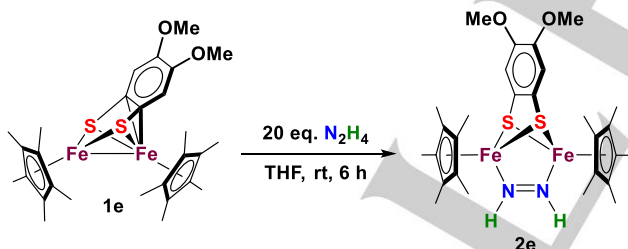
In order to examine the influence of reduction potential on catalytic performance, we chose the biomimetic hydrazine disproportionation as the model reaction. As shown in **Table 2**, we investigated the catalytic activity of complexes **1a-1f** toward the disproportionation of hydrazine at ambient temperature. Using complex **1a** as catalyst, in the presence of 20 equiv. of hydrazine, ammonia was obtained in 36.2% yield (**Table 2, Entry 1**) and N_2 was determined in 39.7% yield by gas chromatography (GC) analysis. In addition, the results of the GC analysis also show only a trace amount of hydrogen was produced during the catalytic cycle. Hence, the hydrazine disproportionation catalyzed by this series of bdt-bridged diiron complexes should occur through a stoichiometric reaction pathway of $3\text{N}_2\text{H}_4 \rightarrow 4\text{NH}_3 + \text{N}_2$ as shown in **Table 2**. When the phenyl ring of the bridging bdt ligand is modified by electron-withdrawing fluoride group, complex **1b** featuring a $\text{Fe}^{\text{II}}\text{Fe}^{\text{II}}/\text{Fe}^{\text{II}}\text{Fe}^{\text{I}}$ redox couple at a higher potential exhibits relatively poor catalytic capability with the ammonia yield of only 27.1% (**Table 2, Entry 2**). Contrarily, when introducing the electron-donating group, the catalytic ability of complexes **1c-1f** with lower redox potential is remarkably enhanced. As shown in **Table 2, Entries 3-6**, the maximum of ammonia yield is 65.6% corresponding to the maximum of turnover number of 13.1, which is comparable to other reported iron complexes.^[10,13c,13d,19] Notably, the changing trend of catalytic activity toward disproportionation of hydrazine is in general accord with variation of the redox potential induced by the substituent modification. As the electron-donating capacity of the substituent on the bdt ligand gradually enhances, the electron density of the iron centers obviously increases, which is helpful to further coordination activation of substrate hydrazine. Hence, the introduction of the electron-donating group can improve the catalytic activity of hydrazine disproportionation. Among these complexes, complex **1f** with the lowest redox potential exhibits the best catalytic ability.

Table 2 Catalytic disproportionation of hydrazine by bdt-bridged diiron complexes **1a-1f**.^[a]

Entry	Catalyst	$E_{1/2}^{\text{red}}$ (V)	NH ₃ /yield (%) ^[b]	N ₂ /yield (%) ^[c]	TON
1	1a	-0.494	36.2	39.7	7.3
2	1b	-0.402	27.1	29.6	5.4
3	1c	-0.848	49.0	54.1	9.8
4	1d	-0.820	59.0	61.5	11.8
5	1e	-0.883	62.4	62.1	12.5
6	1f	-0.920	65.6	67.5	13.1

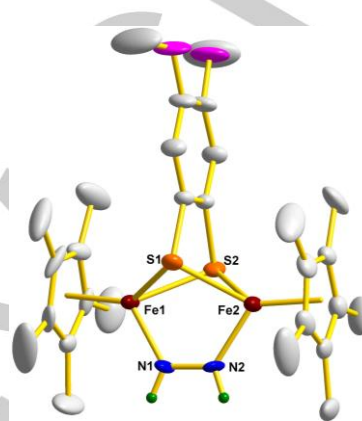
[a] N₂H₄ (0.6 mmol), Cat. (0.03 mmol, 5 mol%), THF (3 mL), rt, 6 h. [b] The yield of NH₃ was determined by ¹H NMR spectroscopy. [c] The yield of N₂ was determined by GC analysis.

One step further, to get insight into the possible mechanism of hydrazine disproportionation promoted by this bdt-bridged diiron system. We attempted to explore the reactivity of bdt-bridged diiron complex toward hydrazine and chose complex **1e** as representative reaction precursor. As shown in **Scheme 2**, treatment of complex **1e** with excess N₂H₄ in THF at room temperature resulted in the generation of a neutral bdt-bridged diiron diazene complex [Cp*Fe(μ-η²:η²-bdt^{2OMe})(μ-η¹:η¹-N₂H₂)FeCp*] (**2e**) in a moderate yield. The ¹H NMR spectrum of complex **2e** shows three intense singlets at 1.36, 3.48 and 6.83 ppm, which are assigned to the methyl protons of the two equivalent Cp* and OMe groups and the two protons of the bdt^{2OMe} ligand. Notably, a diagnostic signal at 14.32 ppm in the low field with the integral area of 2H is attributed to the two protons of the diazene group, which is similar to other diiron diazene complexes.^[16,20] In addition, the infrared (IR) spectrum of **2e** shows one characteristic absorption peak at 3256 cm⁻¹ for N–H stretching vibration, which provides further evidence for the existence of the diazene group.

**Scheme 2.** Reaction of complex **1e** with excess hydrazine.

Above spectroscopic characterizations are fully consistent with its solid-state structure confirmed by X-ray diffraction analysis. As shown in **Figure 3**, a diazene ligand was bridged between the two iron centers in a *cis*-μ-η¹:η¹ coordination pattern. The distance between the two iron centers is 3.2193(13) Å, which suggests there is no metal-metal bonding interaction. The N–N bond length of 1.295(7) Å is similar to those found in known diiron complexes bearing an end-on bridging N₂H₂ ligand (1.300–1.317 Å),^[16,20] which is with evident N(sp²)=N(sp²) double bond character. In addition, the Fe–N bond lengths are 1.821(5) and 1.836(5) Å, which also indicates the sp²-hybridization of nitrogen

atoms in the diazene ligand. Importantly, this diazene species can also be proved to be a catalyst for the disproportionation of hydrazine to release ammonia in 19.6% yield. Obvious difference in ammonia yield suggests the conversion of hydrazine into ammonia promoted by complexes **1e** and **2e** may be different. In other words, complex **2e** may not be involved in the catalytic disproportionation of hydrazine promoted by **1e**.

**Figure 3.** ORTEP (ellipsoids at 50% probability) diagram of bdt^{2OMe}-bridged diiron diazene complex **2e**. The hydrogen atoms except for those on the nitrogen atoms are omitted for clarity.

Conclusions

In summary, through the strategy of substituent modulation, a series of modified bdt-bridged diiron complexes **1b-1f** were synthesized and characterized by spectroscopy and crystallography. As the enhancement of electron-donating capacity, the redox couple of these complexes gradually shifts to more negative potential. Further studies on the catalytic activity toward hydrazine disproportionation indicates the diiron complex with the lowest redox potential exhibits the highest catalytic activity, which is very helpful to design more efficient catalysts for hydrazine disproportionation to release ammonia. Interestingly, a diiron diazene bridged complex was independently synthesized and identified by spectroscopy and X-ray crystallography. As expected, this diazene species **2e** can also serve as a catalyst for hydrazine disproportionation to ammonia, however, the lower catalytic activity indicates that mechanisms other than the one involving **2e** may operate. Further studies on catalytic transformation of N₂ and other nitrogenous substrates using this {Fe₂S₂} platform is underway.

Experimental Section

General Procedures: All manipulations were routinely carried out under an argon atmosphere using standard Schlenk-line techniques. All solvents were dried and distilled over an appropriate drying agent under argon. Anhydrous FeCl₂ (Aldrich), 1,2,3,4-tetrafluorobenzene (Energy Chemical), 4-(*tert*-butyl)benzenethiol (Energy Chemical), 4-methoxybenzenethiol (Energy Chemical), 1,2-dibromo-4,5-dimethoxybenzene (Energy Chemical), 3-bromo-*N,N*-dimethylaniline

(Energy Chemical), ^tBuLi (Energy Chemical), Fc (J&K Scientific) and hydrazine (Aldrich) were used as received without further purification. Bdt-bridged diiron complex [Cp*Fe(μ-η²:η⁴-bdt)FeCp*] (**1a**),^[16] pentamethylcyclopentadiene,^[21] 3,4,5,6-tetrafluorobenzene-1,2-dithiol,^[22] 4-(*tert*-butyl)benzene-1,2-dithiol,^[23] 4,5-dimethoxybenzene-1,2-dithiol^[24] and 4-(dimethylamino)benzene-1,2-dithiol^[25,26] were prepared according to the literatures.

Spectroscopic Measurements: The NMR spectra were recorded on a Brüker 400 Ultra Shield spectrometer or Brüker Ascend 600 spectrometer. The chemical shifts (δ) are given in parts per million relative to CD₂Cl₂ (5.32 ppm for ¹H) or C₆D₆ (7.16 ppm for ¹H). Infrared spectra were recorded on a Nicolet 6700 FT-IR spectrometer. Elemental analyses were performed on a Vario EL analyzer. Gas chromatography was performed with a Techcomp GC7900 gas chromatography instrument with argon as the carrier gas and a thermal conductivity detector.

Electrochemistry: Electrochemical measurements were performed with a BAS-100W electrochemical potentiostat at a scan rate of 100 mV/s. Cyclic voltammetry experiments were carried out in a three-electrode cell under argon at room temperature. The working electrode was a glassy carbon disk (diameter 3 mm), the reference electrode was a nonaqueous Ag/Ag⁺ electrode, the auxiliary electrode was a platinum wire, and the supporting electrolyte was 0.1 M ^tBu₄NPF₆ in CH₂Cl₂. All potentials reported herein are quoted relative to the Fc^{+/0} couple.

X-ray crystallography: Single-crystal X-ray diffraction studies were carried out on a Brüker SMART APEX CCD diffractometer with graphite-monochromated Mo K α radiation ($\lambda = 0.71073$ Å). Empirical absorption corrections were performed using the SADABS program.^[27] All of the structures were solved with the Superflip structure solution program using Charge Flipping and refined with the XL refinement package using Least Squares minimization that implanted in Olex2.^[28] All of the hydrogen atoms were placed at the calculation positions. CCDC depositions 1986574 (**1b**), 1986575 (**1c**), 1986576 (**1d**), 1986577 (**1e**), 1986578 (**1f**) and 2018402 (**2e**) can be obtained free of charge from the Cambridge Crystallographic Data Center. Crystal data and collection details for complexes **1b-f** and **2e** are given in **Table S1**, **Table S2** and **Table S3** in the *Supporting Information*. For **1c**, the bdt^{Bu} ligand was restrained to be similar with the adjacent atoms due to the substitutional disorder, and the "simu" restraint was used with the deviation being 0.02 to help the refinement. For **1d**, the Cp* ligand was restrained to be similar with the adjacent atoms due to the substitutional disorder, and the "simu" restraint was used with the deviation being 0.02 to help the refinement. For **1f**, the bdt^{NMe₂} ligand was restrained to be similar with the adjacent atoms due to the substitutional disorder, and the "simu" restraint was used with the deviation being 0.02 to help the refinement. For **2e**, the Cp* ligand was restrained to be similar with the adjacent atoms due to the substitutional disorder, and the "simu" restraint was used with the deviation being 0.01 to help the refinement. The "delu" restraint was used with the deviation being 0.001 to avoid the Hirshfeld Test Diffon C24–O1 bond. The "isor" restraint was used with the deviation being 0.01 on three carbon atoms.

Synthesis of 4-methoxybenzene-1,2-dithiol: A mixture of *n*-hexane (100 mL), *N,N,N',N'*-tetramethylethylenediamine (10 mL), and 4-methoxybenzenethiol (4.2 g, 30 mmol) was cooled under argon to 0 °C and then treated with 2.5 M ^tBuLi (26 mL, 67 mmol). After being stirred for 24 h, the mixture was added by sublimed sulfur (2.1 g, 67 mmol) at room temperature, and then the suspension was stirred for 12 h. The *n*-hexane was removed *in vacuo* and replaced with an equal volume of THF. The solution was cooled to 0 °C, and LiAlH₄ (1.7 g, 45 mmol) was added cautiously. After the initial exothermic reaction subsided, the

solution was refluxed for 12 h. The solution was cooled to room temperature and poured into cold 2 M HCl (150 mL). The solution was extracted with Et₂O. The combined organic phase was dried with MgSO₄ and concentrated *in vacuo*. The residue was distilled to afford the title compound as colorless oil (1.5 g, 9 mmol, 29%). ¹H NMR (400 MHz, CDCl₃, ppm): δ 7.34 (d, *J* = 8.3 Hz, 1H, bdt-*H*), 6.92 (s, 1H, bdt-*H*), 6.63 (d, *J* = 8.6 Hz, 1H, bdt-*H*), 3.78 (s, 3H, OMe-CH₃).

Synthesis of [Cp*Fe(μ-η²:η⁴-bdt^{4F})FeCp*] (1b**):** To a stirred suspension of Cp*Li (557 mg, 3.92 mmol) in THF (40 mL) was added anhydrous FeCl₂ (498 mg, 3.92 mmol) and stirred at 0 °C for 1 h. The resulting olive-green [Cp*FeCl]₂ suspension was cooled to -78 °C. A suspension of dilithium 3,4,5,6-tetrafluorobenzene-1,2-dithiolate in THF (40 mL), prepared by the reaction of ^tBuLi (1.57 mL, 2.5 M solution in *n*-hexane 3.92 mmol) and 3,4,5,6-tetrafluorobenzene-1,2-dithiol (420 mg, 1.96 mmol) at 0 °C, was cooled to -78 °C and then transferred to a cooled solution of [Cp*FeCl]₂. The mixture was placed in a -78 °C bath for 1 h and stirred overnight as it warmed to room temperature. The resulting red-purple solution was evaporated, and then the residue was extracted with *n*-hexane. After being concentrated and refrigerated at -30 °C, the black crystals of [Cp*Fe(μ-η²:η⁴-bdt^{4F})FeCp*] (**1b**, 240 mg, 0.40 mmol, 20%) were isolated. ¹H NMR (400 MHz, CD₂Cl₂, ppm): δ 1.67 (br, 30H, Cp*-CH₃). IR (KBr, cm⁻¹): 2962, 2906, 1483, 1396, 1261, 1093, 1025, 802. Anal. Calcd. For C₂₆H₃₀Fe₂S₂F₄: C, 52.54; H, 5.09. Found: C, 52.27; H, 5.40.

Synthesis of [Cp*Fe(μ-η²:η⁴-bdt^{Bu})FeCp*] (1c**):** To a stirred suspension of Cp*Li (711 mg, 5.01 mmol) in THF (40 mL) was added anhydrous FeCl₂ (636 mg, 5.01 mmol) and stirred at 0 °C for 1 h. The resulting olive-green [Cp*FeCl]₂ suspension was cooled to -78 °C. A suspension of dilithium 4-(*tert*-butyl)benzene-1,2-dithiolate in THF (40 mL), prepared by the reaction of ^tBuLi (2.0 mL, 2.5 M solution in *n*-hexane, 5.01 mmol) and 4-(*tert*-butyl)benzene-1,2-dithiol (496 mg, 2.51 mmol) at 0 °C, was cooled to -78 °C and then transferred to the cooled solution of [Cp*FeCl]₂. The mixture was placed in a -78 °C bath for 1 h and stirred overnight as it warmed to room temperature. The resulting red-purple solution was evaporated, and then the residue was extracted with *n*-hexane. After being concentrated and refrigerated at -30 °C, the red-black crystals of [Cp*Fe(μ-η²:η⁴-bdt^{Bu})FeCp*] (**1c**, 434 mg, 0.75 mmol, 30%) were isolated. ¹H NMR (600 MHz, C₆D₆, ppm): δ 7.74 (d, *J* = 47.6 Hz, 2H), 6.93 (s, 1H), 1.76 (br, 30H), 1.11 (s, 9H). IR (KBr, cm⁻¹): 2961, 2905, 2868, 1575, 1448, 1394, 1241, 1111, 1020, 814. Anal. Calcd. For C₃₀H₄₂Fe₂S₂: C, 62.29; H, 7.32. Found: C, 62.50; H, 7.45.

Synthesis of [Cp*Fe(μ-η²:η⁴-bdt^{OMe})FeCp*] (1d**):** To a stirred suspension of Cp*Li (636 mg, 4.48 mmol) in THF (40 mL) was added anhydrous FeCl₂ (569 mg, 4.48 mmol) and stirred at 0 °C for 1 h. The resulting olive-green [Cp*FeCl]₂ solution was cooled to -78 °C. A suspension of dilithium 4-methoxybenzene-1,2-dithiolate in THF (40 mL), prepared by the reaction of ^tBuLi (1.8 mL, 2.5 M solution in *n*-hexane, 4.48 mmol) and 4-methoxybenzene-1,2-dithiol (385 mg, 2.24 mmol) at 0 °C, was cooled to -78 °C and then transferred to a cooled solution of [Cp*FeCl]₂. The mixture was placed in a -78 °C bath for 1 h and stirred overnight as it warmed to room temperature. The resulting red-purple solution was evaporated, and then the residue was extracted with *n*-hexane. After being concentrated and refrigerated at -30 °C, the red-black crystals of [Cp*Fe(μ-η²:η⁴-bdt^{OMe})FeCp*] (**1d**, 244 mg, 0.44 mmol, 20%) were isolated. ¹H NMR (400 MHz, C₆D₆, ppm): δ 7.57 (s, 1H, bdt-*H*), 6.92 (s, 1H, bdt-*H*), 6.82 (s, 1H, bdt-*H*), 3.21 (s, 3H, OMe-CH₃), 1.76 (br, 30H, Cp*-CH₃). IR (KBr, cm⁻¹): 2962, 2904, 2856, 1589, 1454, 1373, 1244, 1203, 1045, 1027, 813. Anal. Calcd. For C₂₇H₃₆Fe₂S₂O: C, 58.71; H, 6.57. Found: C, 58.91; H, 6.58.

Synthesis of [Cp*Fe(μ - η^2 : η^4 -bdt^{2OMe})FeCp*] (1e): To a stirred suspension of Cp*Li (506 mg, 3.56 mmol) in THF (40 mL) was added anhydrous FeCl₂ (453 mg, 3.56 mmol) and stirred at 0 °C for 1 h. The resulting olive-green [Cp*FeCl]₂ solution was cooled to -78 °C. A suspension of dilithium 4,5-dimethoxybenzene-1,2-dithiolate in THF (40 mL), prepared by the reaction of ^tBuLi (1.43 mL, 2.5 M solution in *n*-hexane, 3.56 mmol) and 4,5-dimethoxybenzene-1,2-dithiol (360 mg, 1.78 mmol) at 0 °C, was cooled to -78 °C and then transferred to a cooled solution of [Cp*FeCl]₂. The mixture was placed in a -78 °C bath for 1 h and stirred overnight as it warmed to room temperature. The resulting red-purple solution was evaporated, and then the residue was washed with *n*-hexane and extracted with benzene to give a brown powder [Cp*Fe(μ - η^2 : η^4 -bdt^{2OMe})FeCp*] (**1e**, 166 mg, 0.29 mmol, 16%). Crystals suitable for X-ray diffraction were obtained from a THF solution layered with *n*-hexane. ¹H NMR (400 MHz, C₆D₆, ppm): δ 6.87 (s, 2H, bdt-*H*), 3.26 (s, 6H, OMe-*CH*₃), 1.81 (d, *J* = 175.5 Hz, 30H, Cp*-*CH*₃). IR (KBr, cm⁻¹): 2961, 2901, 2854, 1581, 1487, 1434, 1253, 1175, 1037, 828. Anal. Calcd. For C₂₈H₃₈Fe₂S₂O₂: C, 57.74; H, 6.58. Found: C, 57.39; H, 6.48.

Synthesis of [Cp*Fe(μ - η^2 : η^4 -bdt^{NMe2})FeCp*] (1f): To a stirred suspension of Cp*Li (216 mg, 1.52 mmol) in THF (40 mL) was added anhydrous FeCl₂ (193 mg, 1.52 mmol) and stirred at 0 °C for 1 h. The resulting olive-green [Cp*FeCl]₂ solution was cooled to -78 °C. A suspension of dilithium 4-(dimethylamino)benzene-1,2-dithiolate (150 mg, 0.76 mmol) in THF (40 mL) was cooled to -78 °C and then transferred to a cooled solution of [Cp*FeCl]₂. The mixture was placed in a -78 °C bath for 1 h and stirred overnight as it warmed to room temperature. The resulting red-purple solution was evaporated, and then the residue was extracted with *n*-hexane. After being concentrated and refrigerated at -30 °C, the red-black crystals of [Cp*Fe(μ - η^2 : η^4 -bdt^{NMe2})FeCp*] (**1f**, 78 mg, 0.14 mmol, 18%) were isolated. ¹H NMR (400 MHz, C₆D₆, ppm): δ 7.62 (s, 1H, bdt-*H*), 6.81 (s, 1H, bdt-*H*), 6.66 (s, 1H, bdt-*H*), 2.39 (s, 6H, NMe₂-*CH*₃), 1.81 (br, 30H, Cp*-*CH*₃). IR (KBr, cm⁻¹): 2964, 2900, 2854, 1573, 1442, 1374, 1355, 1262, 1099, 1025, 802. Anal. Calcd. For C₂₈H₃₉Fe₂NS₂: C, 59.48; H, 6.95; N, 2.48. Found: C, 59.28; H, 6.75; N, 2.54.

Synthesis of [Cp*Fe(μ - η^2 : η^2 -bdt^{2OMe})(μ - η^1 : η^1 -N₂H₂)FeCp*] (2e): At room temperature, 20 equiv. of N₂H₄ (110 μ L, 3.44 mmol) was added to a stirred solution of complex **1e** (100 mg, 0.18 mmol) in 10 mL THF. After being stirred for 6 h, the solvent was evaporated. The residue was washed with Et₂O (3x3 mL) to give a brown powder [Cp*Fe(μ - η^2 : η^2 -bdt^{2OMe})(μ - η^1 : η^1 -N₂H₂)FeCp*] (**2e**, 55 mg, 0.09 mmol, 50%). Crystals suitable for X-ray diffraction were obtained from a CH₂Cl₂ solution layered with *n*-hexane. ¹H NMR (400 MHz, C₆D₆, ppm): δ 14.32 (s, 2H, NH-*H*), 6.83 (s, 2H, bdt-*H*), 3.48 (s, 6H, OMe-*H*), 1.36 (s, 30H, Cp*-*CH*₃). IR (KBr, cm⁻¹): 3256($\nu_{\text{N-H}}$), 2964, 2905, 2854, 1575, 1464, 1453, 1379, 1251, 1203, 1172, 1037, 774. There is no satisfactory elemental analysis value obtained even though several attempts have been made using high-quality single-crystals of **2e**. This may be caused by incomplete combustion or thermal degradation.

General procedure for catalytic disproportionation of hydrazine: A THF (3 mL) solution of catalyst (0.03 mmol) was placed to a 50 mL Schlenk flask. Then N₂H₄ (19 μ L, 0.6 mmol) was introduced into the stirred solution. After being stirred for 6 h at 25 °C, the reaction volatiles were transferred under reduced pressure into a frozen ethereal solution of HCl (4 M, 3 mL) in a 25 mL Schlenk flask. After thawing, the solution was stirred at room temperature for 15 min. All solvent and excess HCl were removed *in vacuo* to yield colorless solids. ¹H NMR analysis (DMSO-*d*₆) of the resulting colorless solids indicated the presence of NH₄Cl. The NH₄Cl was quantified by integration of the NH₄⁺ resonance with respect to an internal reference of Fc. ¹H NMR (400 MHz, DMSO-*d*₆, ppm) spectrum of NH₄Cl was shown in **Figure S13**.

Acknowledgements

This work was supported by the National Natural Science Foundation of China (No. 21690064, 21571026, 21231003), the Program for Changjiang Scholars and Innovative Research Team in University (No. IRT13008), the "111" project of the Ministry of Education of China and the Fundamental Research Funds for the Central Universities (DUT19RC(3)013).

Keywords: Nitrogenase • Iron • S Ligands • Hydrazine • Substituent effect

Conflicts of interest

The authors declare no competing financial interests.

References

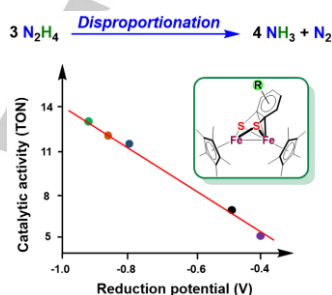
- [1] a) T. M. Buscagan, D. C. Rees, *Joule*. **2019**, *3*, 1–17; b) K. Tanifuji, Y. Ohki, *Chem. Rev.* **2020**, *120*, 5194–251.
- [2] a) J. C. Peters, M. P. Mehn, in *Activation of Small Molecules* (Ed.: W. B. Tolman), Wiley: Weinheim, **2006**; pp. 81–119; b) P. L. Holland, in *Comprehensive Coordination Chemistry II*, Vol. 8 (Eds.: J. A. McCleverty, T. J. Meyer), Elsevier, **2004**; pp. 569–599.
- [3] a) T. Spatzal, K. A. Perez, O. Einsle, J. B. Howard, D. C. Rees, *Science* **2014**, *345*, 1620–1623; b) W. Kang, C. C. Lee, A. J. Jasnowski, M. W. Ribbe, Y. Hu, *Science* **2020**, *368*, 1381–1385.
- [4] a) B. M. Barney, M. Laryukhin, R. Y. Igarashi, H.-I. Lee, P. C. Dos Santos, T.-C. Yang, B. M. Hoffman, D. R. Dean, L. C. Seefeldt, *Biochemistry* **2005**, *44*, 8030–8037; b) D. Lukoyanov, S. A. Dikanov, Z.-Y. Yang, B. M. Barney, R. I. Samoilova, K. V. Narasimhulu, D. R. Dean, L. C. Seefeldt, B. M. Hoffman, *J. Am. Chem. Soc.* **2011**, *133*, 11655–11664.
- [5] L. C. Seefeldt, Z.-Y. Yang, D. A. Lukoyanov, D. F. Harris, D. R. Dean, S. Raugel, B. M. Hoffman, *Chem. Rev.* **2020**, *120*, 5082–5106.
- [6] L. Davis, *Arch. Biochem. Biophys.* **1980**, *204*, 270–276.
- [7] a) E. Block, G. Ofori-Okai, H. Kang, J. Zubieta, *J. Am. Chem. Soc.* **1992**, *114*, 758–759; b) P. Schollhammer, F. Y. Pétillon, S. Pöder-Guillou, J. Y. Saillard, J. Talarmin, K. W. Muir, *Chem. Commun.* **1996**, *23*, 2633–2634; c) P. B. Hitchcock, D. L. Hughes, M. J. Maguire, K. Marjani, R. L. Richards, *J. Chem. Soc., Dalton Trans.* **1997**, 4747–4752.
- [8] R. R. Schrock, T. E. Glassman, M. G. Vale, M. Kol, *J. Am. Chem. Soc.* **1993**, *115*, 1760–1772.
- [9] a) S. M. Malinak, K. D. Demadis, D. Coucouvanis, *J. Am. Chem. Soc.* **1995**, *117*, 3126–3133; b) W.-C. Chu, C.-C. Wu, H.-F. Hsu, *Inorg. Chem.* **2006**, *45*, 3164–3166.
- [10] K. Umehara, S. Kuwata, T. Ikariya, *J. Am. Chem. Soc.* **2013**, *135*, 6754–6757.
- [11] a) S. Kuwata, Y. Mizobe, M. Hidai, *Inorg. Chem.* **1994**, *33*, 3619–3620; b) D. Sellmann, A. Hille, A. Rösler, F. W. Heinemann, M. Moll, G. Brehm, S. Schneider, M. Reiher, B. A. Hess, W. Bauer, *Chem. Eur. J.* **2004**, *10*, 819–830; c) S. S. Rozenel, J. Arnold, *Inorg. Chem.* **2012**, *51*, 9730–9739.
- [12] a) S. M. Malinak, D. Coucouvanis, *Prog. Inorg. Chem.* **2001**, *49*, 599–662; b) I. Takei, K. Dohki, K. Kobayashi, T. Suzuki, M. Hidai, *Inorg. Chem.* **2005**, *44*, 3768–3770; c) B. Wu, K. M. Gramigna, M. W. Bezpalko, B. M. Foxman, C. M. Thomas, *Inorg. Chem.* **2015**, *54*, 10909–10917; d) N. X. Gu, G. Ung, J. C. Peters, *Chem. Commun.* **2019**, *55*, 5363–5366.
- [13] a) Y. Chen, Y. Zhou, P. Chen, Y. Tao, Y. Li, J. Qu, *J. Am. Chem. Soc.* **2008**, *130*, 15250–15251; b) Y.-H. Chang, P.-M. Chan, Y.-F. Tsai, G.-H. Lee, H.-F. Hsu, *Inorg. Chem.* **2014**, *53*, 664–666; c) S. E. Creutz, J. C.

- Peters, *J. Am. Chem. Soc.* **2015**, *137*, 7310–7313; d) L. Su, D. Yang, B. Wang, J. Qu, *Inorg. Chem. Commun.* **2020**, *112*, 107735.
- [14] S. Sproules, K. Wieghardt, *Coord. Chem. Rev.* **2010**, *254*, 1358–1382.
- [15] a) E. S. Donovan, J. J. McCormick, G. S. Nichol, G. A. N. Felton, *Organometallics* **2012**, *31*, 8067–8070; b) S. C. Eady, M. M. MacInnes, N. Lehnert, *Inorg. Chem.* **2017**, *56*, 11654–11667.
- [16] Y. Li, Y. Li, B. Wang, Y. Luo, D. Yang, P. Tong, J. Zhao, L. Luo, Y. Zhou, S. Chen, F. Cheng, J. Qu, *Nat. Chem.* **2013**, *5*, 320–326.
- [17] K. Ray, E. Bill, T. Weyhermüller, K. Wieghardt, *J. Am. Chem. Soc.* **2005**, *127*, 5641–5654.
- [18] D. Yang, Y. Li, B. Wang, X. Zhao, L. Su, S. Chen, P. Tong, Y. Luo, J. Qu, *Inorg. Chem.* **2015**, *54*, 10243–10249.
- [19] Y. Zhang, J. Zhao, D. Yang, Y. Zhang, B. Wang, J. Qu, *Inorg. Chem. Commun.* **2017**, *83*, 66–69.
- [20] a) D. Sellmann, W. Soglowek, F. Knoch, M. Moll, *Angew. Chem. Int. Ed.* **1989**, *28*, 1271–1272; b) Y. Chen, L. Liu, Y. Peng, P. Chen, Y. Luo, J. Qu, *J. Am. Chem. Soc.* **2011**, *133*, 1147–1149; c) C. T. Saouma, C. E. Moore, A. L. Rheingold, J. C. Peters, *Inorg. Chem.* **2011**, *50*, 11285–11287.
- [21] C. M. Fendrick, L. D. Schertz, E. A. Mintz, T. J. Marks, T. E. Bitterwolf, P. A. Horine, T. L. Hubler, J. A. Sheldon, D. D. Belin, *Inorg. Synth.* **1992**, *29*, 193–198.
- [22] M. J. Koh, R. K. M. Khan, S. Torker, M. Yu, M. S. Mikus, A. H. Hoveyda, *Nature* **2015**, *517*, 181–186.
- [23] E. Block, V. Eswarakrishnan, M. Gernon, G. Ofori-Okai, C. Saha, K. Tang, J. Zubieta, *J. Am. Chem. Soc.* **1989**, *111*, 658–665.
- [24] A. Döring, C. Fischer, C. Schulzke, *Z. Anorg. Allg. Chem.* **2013**, *639*, 1552–1558.
- [25] H. Reed, T. R. Paul, W. J. Chai, *J. Org. Chem.* **2018**, *83*, 11359–11368.
- [26] I. Tabushi, K. Yamamura, H. Nonoguchi, *Chem. Lett.* **1987**, *16*, 1373–1376.
- [27] G. M. Sheldrick, SADABS, *Program for area detector adsorption correction*; Institute for Inorganic Chemistry, University of Göttingen, Germany, 1996.
- [28] a) L. Palatinus, G. Chapuis, *J. Appl. Crystallogr.* **2007**, *40*, 786–790; b) O. V. Dolomanov, L. J. Bourhis, R. J. Gildea, J. A. Howard, H. Puschmann, *J. Appl. Crystallogr.* **2009**, *42*, 339–341; c) G. M. Sheldrick, *Acta Crystallographica Section C: Structural Chemistry*, **2015**, *71*, 3–8.

Key Topic

Bioinorganic Chemistry

TOC



The substituent modulation of the redox non-innocent benzene-1,2-dithiolate ligand has an obvious effect on the catalytic activity of hydrazine disproportionation to ammonia promoted by biomimetic diiron nitrogenase model complexes with different reduction potentials.